Journal of Ambient Intelligence and Smart Environments 9 (2017) 181–191
DOI 10.3233/AIS-170425
IOS Press

Estimation of human walking speed by Doppler radar for elderly care

Liyang Rui [a], Shanjie Chen [a], K.C. Ho [a,*], Marilyn Rantz [b] and Marjorie Skubic [a]
[a] *Department of Electrical Engineering and Computer Science, University of Missouri, Columbia, MO, USA*
E-mails: steve.rui1983@gmail.com, sjchen1984@gmail.com, hod@missouri.edu, skubicm@missouri.edu
[b] *Sinclair School of Nursing, University of Missouri, Columbia, MO, USA*
E-mail: rantzm@missouri.edu

Abstract. This paper presents a human walking speed estimation algorithm using a Doppler radar system for in-home passive gait assessment of elderly adults. The Fast Fourier Transform (FFT) has been a common approach to obtain the gait speed estimation. The proposed algorithm analyzes the received radar signal by counting its zero-crossing periods in the time domain and applies an interquartile range filter to improve its robustness with respect to the gait signature dynamics in the radar data. The proposed algorithm provides better accuracy and does not seem to produce extreme incorrect speed estimates compared to the previously developed FFT method. It has been applied to the Doppler radar system that is deployed in in-home environments to continuously monitor the daily activities of the senior residences and estimate their gait speeds. Improving the accuracy of gait parameters can better facilitate the assessment of the physical conditions of the seniors.

Keywords: Doppler radar, short time Fourier transform, zero-crossing, gait, eldercare

1. Introduction

An in-home health monitoring system is beneficial to improving the life quality of elderly people by detecting harmful events [4,21] and continuously assessing the physical condition of the seniors [10,35,36,43,44]. Researchers [16,22,31] have shown that gait characteristics are important indicators in the assessment and diagnosis of frailty and fall risks of elderly adults. [24] found that the gait velocity is an important predictor of adverse events when the elderly adults are in good condition. [8] showed gait velocity slowing precedes cognitive impairment. The daily walking speed measurements have been indicated to be better able to predict the score of the physical performance of the seniors than the traditional instruments, such as Habitual Gait Speed (HGS) [24], Timed-Up and Go (TUG) [27], and Short Physical Performance Battery (SPPB) [41]. Therefore, continuous gait measurements based on the in-home walking activities of seniors can draw the trends of their gait profiles over time and imply potential health risk [28]. The typical gait monitoring systems are based on video [1,15,17,23,46], wearable sensors [14,33,38], and Doppler radars [13,20,32,39]. Comparing to other sensors, the Doppler radar is attractive because it can detect and measure any movement in the presence of stationary clutter at the background. It provides a more comfortable perception to the elderly compared to the vision based sensors including Kinect since it has the ability to penetrate structures and can hide inside a furniture item or behind a wall. It does not raise the privacy issue for in-home monitoring and avoids the inconvenience caused by the wearable devices [10]. A Doppler radar can sense the motion in the direction between the radar and the subject only and may not have a wide viewing angle. These concerns could be handled by using a few Doppler radars distributed at several locations or positioning the system at the end of a hallway that naturally constrains the walking path.

The possibility of integrating a Doppler radar into an in-home elder care monitoring system has been inves-

*Corresponding author. E-mail: hod@missouri.edu.

tigated in the lab environment in [9,43,45] with positive results reported. The goal of such a system is to track the change of gait characteristics over time and detect the rise of fall risks based on the measurements from the daily in-home activities of the elderly adults so that effective health care can be adopted early to reduce adverse events. The operating environment we assumed in this work is a single person in the viewing range of a Doppler radar and the identity of the person is known. Such an environment is typical in a senior residence apartment. In this study, we propose a walking speed estimation algorithm for elderly adults based on Doppler signatures and evaluate its performance in realistic in-home environments of the seniors. Unlike the traditional spectrogram based algorithm [43,45], this method explores the Doppler signatures in time domain, analyzes their dynamics by short time zero-crossing (STZC) and employs an interquartile range filter to combat the environmental disturbance, yielding more reliable and accurate results. Its robustness is first investigated in a lab environment case study when the highly accurate video based tracking system, Vicon, is served as ground truth. In addition, we discuss the effect of Doppler angle [40] on the gait speed estimation. The proposed method has been implemented in a realistic in-home elder care scenario and its performance is evaluated.

The paper is organized as follows. Section 2 briefly presents related work. Section 3 describes the function and setting of the Doppler radar used in the study along with a summary about the Vicon system and Kinect sensor which serve as the ground truths. Section 4 proposes the gait speed estimation method. Section 5 analyzes its robustness by lab experiments and discusses the effect of the Doppler angle. Section 6 evaluates its performance based on the measurements captured from real in-home activities of many seniors. Section 7 concludes the paper.

2. Related work

Traditionally, trained health care givers assess the walking ability of elderly people in an outpatient setting. In addition to high cost, the accuracy of such method is inconsistent, which is mainly caused by the test environment [2], experience level of the assessor [7,19], as well as the emotional state of the subject [44]. It would be more attractive using an in-home monitoring system that can automatically measure and monitor the gait characteristics of seniors from their daily activities.

The video based methods have been widely investigated for human activity analysis. Specifically for the purpose of elder care, Wang *et al.* [44], proposed an indoor webcam-based system to estimate the gait characters of seniors including walking speed, stride time and stride length. Similar functions are realized in [35] by using the Kinect sensor. Both of them show good estimation accuracies. However, the implementation of a visual system has many limitations, such as lighting condition, occlusion, and the privacy concerns. Some researchers utilized wearable devices to monitor the senior adult activities. [33] performed indoor localization of residents by using a RFID sensor. [14] took advantage of a smart device, which may be already owned by the residents, and used the built-in accelerometer to obtain gait parameters. [38] investigated the potential of gait characterization by Fitbit wristband. The major problem of wearable device based solution is that carrying a device for long time might not be favored by the seniors, especially when they do not feel well [10].

An emerging solution for the human gait analysis is to use the Doppler radar. The appearance of Doppler signatures in the radar returns caused by human motions has been investigated based on time-frequency analysis in [13,20,32,39]. Otero [25] designed a simple, binary classifier to detect if a person is present. [3,5,34] further proposed classifiers to distinguish humans from animals and other objects. Kim and Ling [18] designed a support vector machine to identify different human activities such as walking, running, crawling from the Doppler signatures. [26] focused on the gait analysis and proposed a classifier to distinguish walking from all the other activities. Yardibi *et al.* estimated the human walking speed by computing the short time Fourier transform (STFT) of the radar signal and obtained good accuracy in the lab experiments [45]. They also compared the results from radar with those from the staff performing fall risk assessment [9]. [43] further investigated the performance of the method in [9,45] by evaluating the effect of Doppler angle by laboratory experiments.

In this paper, we extend the study from the lab environment [9,43,45] to the actual residences of the senior adults. Comparing to the lab condition, the actual living environment is more complex. We implement the classifier in [26] to distinguish walks from other human activities, develop a new gait speed estimation al-

gorithm and evaluate its performance in the complex residential environments.

3. Systems

3.1. Pulse-Doppler radar

The Doppler radar used in this study is a pulse-Doppler radar. The proposed algorithm is applicable to other forms of the Doppler radar such as continuous wave. The pulse-Doppler radar in this study has a carrier frequency of 5.8 GHz, a pulse repetition frequency of 10 MHz and a duty cycle of 40%. It has a 20 feet observation range and a 90 degree viewing angle [29]. The radar continuously sends out signal and mixes it with the received echo. It then produces the output after a low pass filter. The radar output is digitalized and collected by a DI-710 data logger from the DATAQ Instruments, Inc. with a sampling frequency f_s of 960 Hz and an A/D resolution of 14 bits [11]. The digital radar data are transmitted to the computer through a Wi-Fi network for further analysis.

The radars were concealed in a wooden box with a height of 0.15 m above the floor as shown in Fig. 1. The radar system was placed in the living room of each senior resident and continuously observed the human motion 24 hours everyday. The walking classifier proposed in [26] was implemented in this study to extract the radar data segments corresponding to human walks.

Fig. 1. The radar system. The figure on the left is the wooden box which contains the radar, data logger and the wireless router. The figure on the right shows their deployment inside the box. They are the data logger, Doppler radar and wireless router from left to right.

3.2. Vicon

The Vicon [42] is a highly accurate human motion capture system. The system measures the 3D coordinates of the reflective markers on the elbows, shoulders, knees, chest and back of the human subjects at a rate of 100 frames per second [42]. The system has been installed in the lab and it serves to provide the ground truth of human walking speed for evaluation. To compute the ground truth, it divides the distance travelled by the back marker in the 2D (x and y) coordinates by the duration of the walk.

3.3. Kinect

The Kinect system was released by the Microsoft with the original purpose for controller free video gaming. It has been successfully developed to be an in-home gait assessment system by Stone *et al.* [35], which estimates the walking speeds and stride lengths of senior subjects with high accuracy. It provides the ground truth data of the walking speeds of the senior subjects in the residential experiments. Similar to the radar system, the Kinect sensor is installed in the living rooms of several senior residents at physically separated locations. It is placed on a shelf beside the main door with a height of 2.75 m (a few centimetres below the ceiling) as shown in Fig. 2. Note that the position relationships between the radar and the Kinect are not the same among different elderly residents due to the diversity of their home configurations. But their 3D coordinates have been measured before data collection.

Fig. 2. The Kinect system.

4. Methodology

The estimation of walking speed uses the frequency change between the transmit and the receive radar signal due to the Doppler effect. The relationship between the frequency shift in radar output f_r and the walking speed v_{Doppler} in the direction along the radar and the object is [30]

$$v_{\text{Doppler}} = c \times f_r/(2f_c), \tag{1}$$

where c is the speed of light, f_c is the carrier frequency that is equal to 5.8 GHz for the radar we use.

This section proposes STZC, which is a method operating in the time domain to estimate the walking speed from the Doppler radar signal. We shall begin with the pre-processing of the radar data and then present the STZC method. A short review of the frequency domain based STFT method [43,45] will be given to contrast the difference with our approach and form the basis for performance study in Sections 5 and 6.

4.1. Pre-processing of radar data

The purpose of the pre-processing is to reduce the noise and interference in the data before applying a speed estimation algorithm. The pre-processing passes the data through an order 10 Butterworth bandpass filter with the passband over $[5, 60]$ Hz. It essentially eliminates the frequency components that are not caused by the walking speed. According to (1) this frequency range corresponds to a speed range of $[0.13, 1.56]$ m/s, which represents a reasonable level of senior walking speed expected.

Figure 3 shows the spectrogram of a typical walking data series before and after passing through the Butterworth bandpass filter. In Fig. 3(a), the dynamic behavior of the spectral content is very obvious from the gait characteristics. The radar data have high frequency components caused by leg motions and low frequency components resulted from torso motions [9,25]. The low frequency components often have greater energy since the torso has larger reflection area. Figure 3(b) indicates the pre-processing by the bandpass filter effectively reduces the effect of leg motions and preserves the torso motion information.

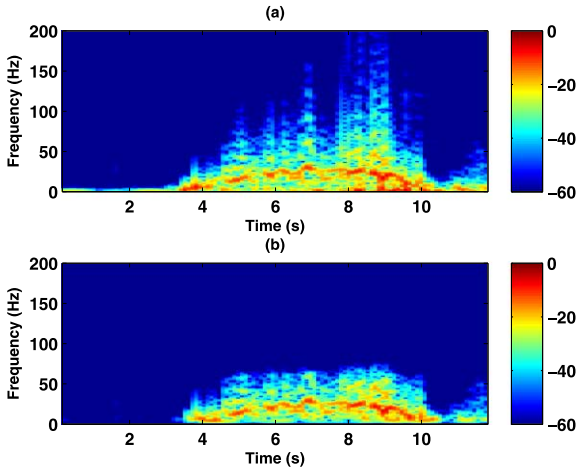

Fig. 3. Spectrogram of a typical series of radar data containing a human walk. (a) Before bandpass filtering; (b) After bandpass filtering. Note that the x and y axes have been converted to the continuous time and frequency domains.

4.2. The STZC method

The STZC method estimates the walking speed by analyzing the dynamics of the radar data in the time domain using three steps.

4.2.1. First step

The first step processing divides the pre-processed radar data into M small segments of 400 samples each through the Hanning window with 75% overlap, where M is the number of total small segments. As shown in [9,43,45], the 400 samples segment length is an appropriate choice. At 960 Hz sampling, each segment corresponds to $400/960 = 0.4167$ s. For example, Fig. 4(a) plots the 59th segment of the same radar data in Fig. 3 (around 6.04 s). It clearly shows the harmonic pattern caused by human walk. We shall denote the mth segment as $x_m(n)$, $n = 1, 2, \ldots, 400$ and $m = 1, 2, \ldots, M$.

4.2.2. Second step

For each segment we generate the zero-crossing series $y_m(n)$, by

$$y_m(n) = \left|\text{sgn}\big(x_m(n)\big) - \text{sgn}\big(x_m(n-1)\big)\right| \quad n = 1, 2, \ldots, 400, \tag{2}$$

where $x_m(0) = 0$ and $\text{sgn}(\bullet)$ is the signum function

$$\text{sgn}\big(x(n)\big) = \begin{cases} 1, & (\bullet) \geq 0, \\ 0, & (\bullet) < 0. \end{cases} \tag{3}$$

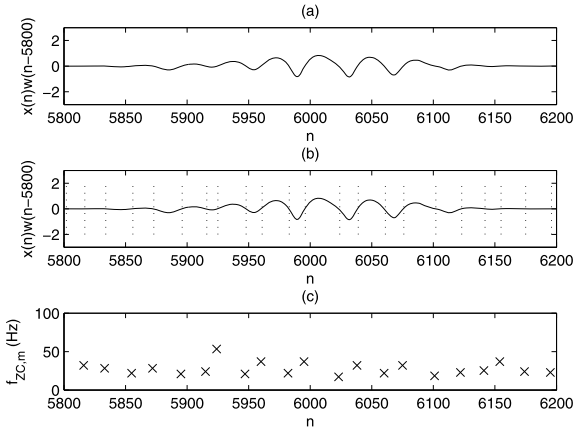

Fig. 4. Illustration of the STZC method. (a) A windowed radar data segment from the first processing step. (b) The radar data segment with zero-crossing points identified by n_l in the second processing step. (c) The individual zero-crossing frequency estimates from the second step.

The index n in which $y_m(n) = 1$ indicates the location at which a sign change in $x_m(n)$ occurs. Figure 4(b) highlights the zero-crossing points in Fig. 4(a).

Suppose there are $L+1$ zero-crossings that occur at indices n_l, $l = 1, 2, \ldots, L+1$. According to [6], we can obtain L zero-crossing frequency estimates in the mth segment by

$$f_{\mathrm{ZC},m}(l) = f_s(n_{l+1} - n_l)^{-1}/2. \tag{4}$$

Figure 4(c) shows the estimated zero-crossing frequencies between each pair of zero-crossing points. The dynamic characteristics of the radar data cause the zero-crossing frequency estimates vary significantly in time. To improve the robustness in the speed estimate, we sort $f_{\mathrm{ZC},m}(l)$ in ascending order and discard the lower and the upper 25%. The frequency estimate resulted from the torso motion in the mth segment is set as the harmonic mean of the remaining, and it is denoted as $\widetilde{f}_{\mathrm{ZC},m}$.

4.2.3. Third step

Finally, the mean of $\widetilde{f}_{\mathrm{ZC},m}$, $m = 1, 2, \ldots, M$, is put into (1) to compute the walking speed as

$$v_{\mathrm{STZC}} = c \times \left(\frac{1}{M} \sum_{m=1}^{M} \widetilde{f}_{\mathrm{ZC},m} \right) \Big/ (2 f_c). \tag{5}$$

4.3. The STFT method

The STFT method [9,43,45] was designed to determine the gait speed from the frequency domain. It also contains three steps.

4.3.1. First step

It is identical to the first step in the STZC method by segmenting the data into M segments.

4.3.2. Second step

The second step applies FFT to each segment and set the frequency estimate of the mth segment as the location of the spectral peak in the first half. That is,

$$f_{\mathrm{FT},m} = (f_s/N) \times \arg \max_{k=0,1,\ldots,N/2-1} \left| \mathrm{FFT}\big(x_m(n)\big) \right|, \tag{6}$$

where $f_s = 960$ Hz is the sampling frequency, $N = 400$ is the segment size and k is the frequency index.

4.3.3. Third step

The third step computes the average of the overall frequency estimates $f_{\mathrm{FT},m}$ from the M segments and converts it to velocity using (1):

$$v_{\mathrm{STFT}} = c \times \left(\frac{1}{M} \sum_{m=1}^{M} f_{\mathrm{FT},m} \right) \Big/ (2 f_c). \tag{7}$$

To improve the estimation result, the STFT method is repeated twice for the purpose of adjusting the preprocessing filter bandwidth according to the overall frequency estimate obtained in the first time [9].

5. Analysis

We would like to contrast the benefit of the proposed method with respect to the STFT technique. The proposed method is expected to be more robust in dealing with the undesirable variations in the data.

The Fourier transform is a very powerful tool to analyze the frequency content of a signal that is stationary. The radar output is expected to be a harmonic signal at the Doppler frequency. In practical scenarios, the radar data has significant amount of modulation in the amplitude caused by the motion and reflections. The amplitude modulation creates additional frequency components, dilutes the Doppler frequency spectral peak and could produce false peaks, making the speed estimate from the STFT approach less accurate.

The proposed technique looks into zero-crossing to estimate the Doppler frequency. It ignores the variations in the amplitude and is resilient to the amplitude modulation effect. Furthermore, we apply the interquartile range filter to eliminate the outliers in the zero-crossing intervals caused by the noise and other undesirable variations in the data. Hence we expect a more reliable result by the proposed method.

A laboratory experiment was conducted. As illustrated in Fig. 5, a male subject walked towards and then away from the radar. The Vicon system recorded the walking trajectory for providing the ground truth. When the radar observes a human walk, it receives a mixture of the reflections from different parts of the subject [13], such as arm, torso and leg. The motion and reflection create amplitude modulation and undesirable frequency components as can be observed in Fig. 6 which depicts the 61st and 72nd segments of the radar data. Figure 7 gives the FFT magnitude spectra of the two segments. The spectrum in Fig. 7(a) gives the correct frequency estimate for the 61st segment. A strong false peak occurs in the spectrum in Fig. 7(b) for the 72nd segment, yielding an incorrect and very far away frequency estimate.

Figure 8 gives the values of the inverse of zero-crossing intervals $f_{ZC,m(l)}$ for the two segments from the second step of the proposed STZC method. The values vary considerably due to the dynamic nature in the data. The interquartile range filter eliminates the extreme values and the frequency estimate in the segment is shown in dotted line. It matches with the ground truth very well for the 61st segment, and is slightly off for the other segment.

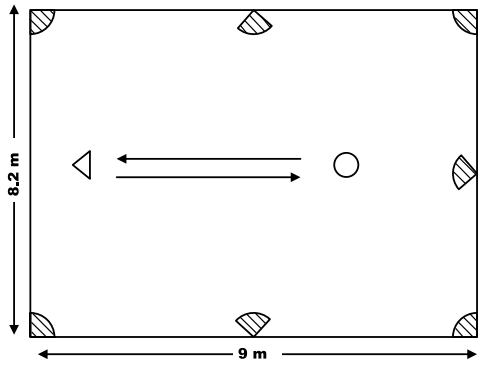

Fig. 5. Layout of the laboratory experiment. The shadowed sectors are the Vicon sensors whose heights are 3 m. The circle represents a male human with height 1.75 m, and the triangle represents the Doppler radar that is 0.15 m above the floor.

Figure 9 shows the walking speed estimates by the STFT and STZC methods from each segment over a duration of 4 s. We have about 38 estimates in each since the 400 sample segment is advanced each time by 100 samples (about 104 ms). Most of the time both methods are able to provide accurate estimates. The STFT method sometimes produces extreme outlier values at some segments. On the other hand the STZC method does not experience this behavior and produces reasonably good estimates in those segments.

Another drawback of the STFT method is that it may not be able to produce a speed estimate when the walking speed varies within a segment. The Fourier analysis assumes a stationary signal and a varying speed segment will not yield a strong harmonic peak in the

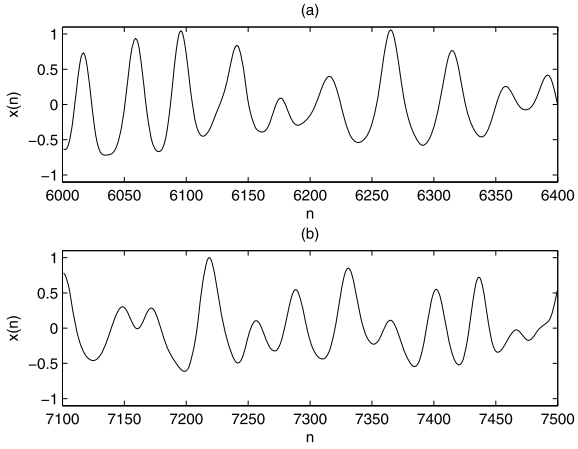

Fig. 6. Radar data of the laboratory experiment. (a) The 61st segment (6.25 s). (b) The 72nd segment (7.40 s).

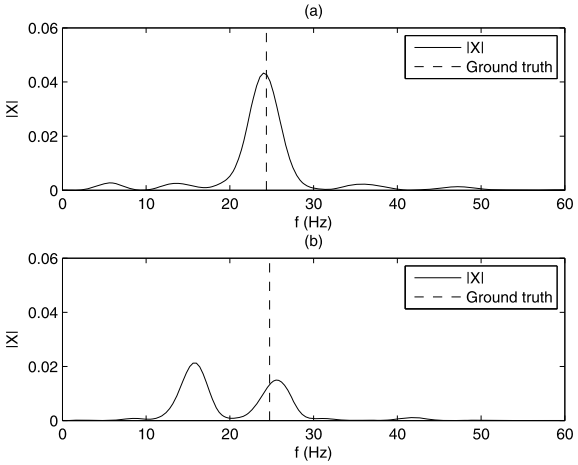

Fig. 7. Robustness analysis of STFT method. (a) Spectrum of the 61st segment (6.25 s). (b) Spectrum of the 72nd segment (7.40 s).

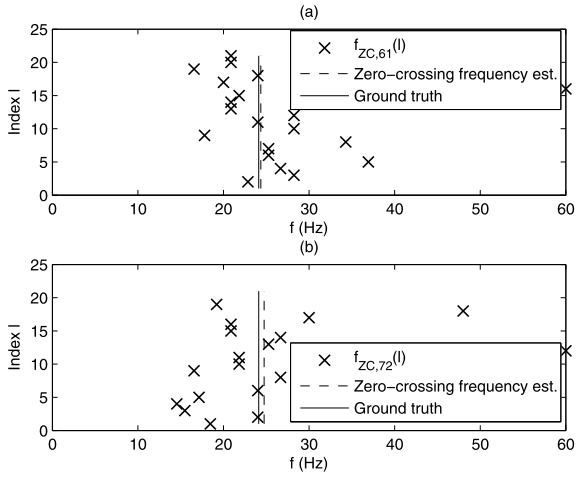

Fig. 8. Robustness analysis of STZC method. (a) Zero-crossing frequency estimates of the 61st segment (6.25 s). (b) Zero-crossing frequency estimates of the 72nd segment (7.40 s).

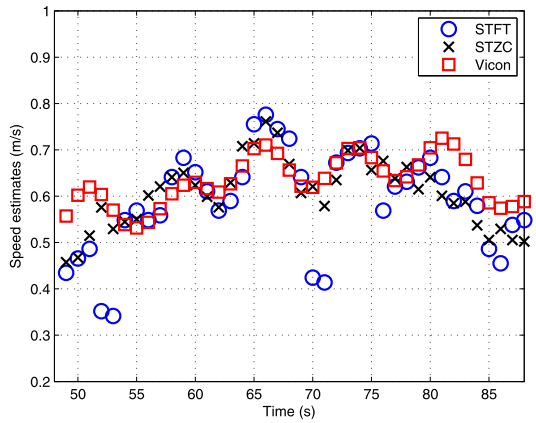

Fig. 9. Performance of th STFT and STZC methods in the lab experiment.

FFT magnitude spectrum to produce the Doppler frequency estimate. The proposed STZC method does not have this problem because it estimates the Doppler frequency within a segment in the time domain. We expect in such a segment with high speed variation, the STZC method as described in Section 4.2 will yield an average speed estimate within the segment.

Table 1 illustrates the root mean square errors (RMSEs) of the STZC and STFT algorithms for the segments of 8 walks collected in the lab environment. The STZC outperforms STFT for all of the walks. Table 2 shows the maximum absolute errors for the same 8 walks and provides similar observations. Tables 1–2 illustrate that the STZC method provides considerable improvement in RMSE and significant improvement

Table 1

RMSEs of STZC and STFT in lab environment using Vicon as ground truth, the unit is m/s

Walk ID	Root mean square error		
	STZC	STFT	Reduction %
1	0.108	0.187	42.24
2	0.084	0.133	36.84
3	0.056	0.094	40.42
4	0.072	0.099	27.27
5	0.060	0.091	34.06
6	0.063	0.075	16.00
7	0.066	0.142	53.52
8	0.095	0.130	26.92

Table 2

Maximum absolute errors of STZC and STFT in lab environment using Vicon as ground truth, the unit is m/s

Walk ID	Maximum absolute error		
	STZC	STFT	Reduction %
1	0.223	0.480	53.54
2	0.193	0.261	26.05
3	0.141	0.260	45.77
4	0.140	0.274	48.90
5	0.135	0.252	46.43
6	0.152	0.232	34.48
7	0.221	0.384	42.45
8	0.193	0.392	50.77

in maximum absolute error. Improvement in the maximum absolute error will reduce false alarms in triggering an alert to the caregivers in which a fatal event such as falling down may have occurred.

The STZC method is applicable for a single moving subject and has a limitation of estimating the speeds when multiple human subjects are present. The STFT method may be able to provide reasonable speed estimates when the Doppler components created by different people are widely separated in the frequency domain [6]. The STZC may not be suitable if the subject is living with his/her family. In addition, STZC may not provide good estimates if the signal-to-noise ratio is low.

5.1. *The effect of Doppler angle*

According to the principle of Doppler effect, the radar can only detect the relative speed component along the direction between the radar and human. If the true gait speed is v_{true} and the angle between the velocity vector and the radar with respect to the object is θ as shown in Fig. 10, the observed walking speed

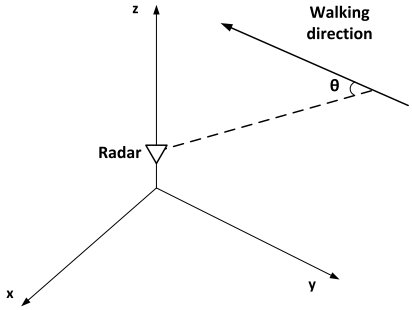

Fig. 10. Illustration of Doppler angle.

Table 3
RMSEs of STZC and STFT, the unit is m/s

ID	Num. segments	Root mean square error		
		STZC	STFT	Reduction %
1	2038	0.13	0.15	13.33
2	2409	0.16	0.17	5.88
3	499	0.12	0.12	0
4	241	0.11	0.12	8.33
5	1415	0.13	0.14	7.14
6	1752	0.11	0.12	8.33
7	3328	0.09	0.10	10.00
8	130	0.15	0.16	6.25

from the radar is [40]

$$v_{\text{Doppler}} = v_{\text{true}} \times \cos\theta. \tag{8}$$

Note that θ is changing during the walk. It is necessary to take this Doppler angle into account when evaluating the gait speed estimates from different methods applied to the radar data [43]. The detail of obtaining the Doppler angle in the performance evaluation is explained in the next section.

6. Experimental results

To further evaluate STZC in a practical scenario, we conducted experiments in the apartments of the senior residence TigerPlace, a senior adult living community in Columbia, Missouri. The experiments and data collections from human subjects were approved by the Institutional Review Board (IRB) at the University of Missouri. The radar data were collected from 8 seniors during January 1, and March 31, 2012 and the number of walking segments available for the performance evaluation is shown in Table 3. The radar and Kinect are installed in the living room of each subject

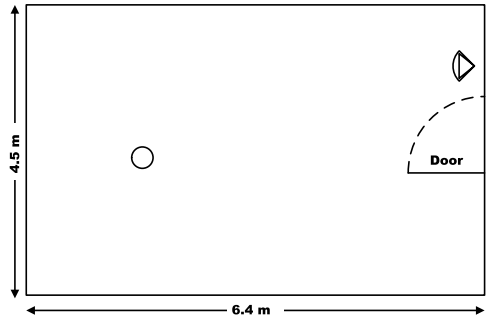

Fig. 11. Layout of the residence experiment of subject #1. The sector and triangle represent the Kinect and radar respectively which are at the same horizontal position. The Kinect is 2.7 m while radar 0.15 m above the ground. The circle represents the subject who generates daily walk behaviors. The locations of the radars and Kinects in the residences of other subjects may be different.

Table 4
Reflective correlation coefficient of the estimated gait speeds with respect to the ground truth v_{Doppler}

ID	Reflective correlation coefficient		
	v_{STZC}	v_{STFT}	v_{Doppler}
1	0.979	0.972	1
2	0.958	0.946	1
3	0.948	0.943	1
4	0.951	0.947	1
5	0.954	0.946	1
6	0.962	0.954	1
7	0.974	0.969	1
8	0.961	0.954	1

and they are not necessarily placed at the same location for different apartments, depending on the configurations of the apartments. Fig. 11 shows the layout of subject 1 as an example. We used the speed estimates from the Kinect [36] as the ground truths for the evaluation of the performance of STZC and STFT methods. The ground truths are derived from the Kinect sensor since we were not able to install the Vicon system in the senior residence apartments. The Kinect sensor has a resolution limited to cm and may have some level of inaccuracy in the obtained speed. They should be taken into account when examining the results in Tables 3–4. Only the data portions detected as walks by both the radar [26] and the Kinect [36] are used for evaluations.

To compensate the effect of Doppler angle in (8), the starting and ending positions of a resident in 3D from each walk are obtained from the Kinect image [35]. Given the radar and Kinect positions and the gait speed estimates from the Kinect, the Doppler angle θ during

the walk can be deduced from the geometry [12]. Due to the limitation of the radar coverage area, only the walks with $\theta < 60^\circ$ are used in the evaluation. The real walking speed v_{true} is obtained using the Kinect [36]. The ground truth v_{Doppler}, which is the physical quantity that can be detected by the Doppler radar, is calculated using (8).

Table 3 summarizes of the RMSEs of the two walking speed estimation algorithms (STZC and STFT). Both methods show good estimation accuracy while the STZC outperforms the STFT with smaller error for most of the eight subjects. This observation is consistent to the theoretical analysis in Sections 4 and 5. The improvement is not as large as in the lab experiment. Part of the reason could come from the detection of the walking segments, as well as the quality of the ground truths derived from the Kinect. Nevertheless, the improvement of RMSE is at least 5% for most subjects as illustrated in Table 3.

Table 4 summarizes their reflective correlation coefficients and indicates that STFT and STZC are highly correlated to the ground truth.

In the proposed STZC method, the interquartile filter provides the robustness of the speed estimate by eliminating unreasonable zero-crossing values due to noise or signal distortion. It appears the Doppler angle estimation is the component that requires further improvement. The angle estimates for the results presented are based on the Kinect image which has a position accuracy in the order of cm only [35,36].

The recent research study [37] has shown that the daily walking speed is able to predict the scores of the traditional individual physical performance instruments, such as HGS, TUG, and SPPB. However, it also exposes the prediction performance of the physical score is sensitive and influenced by the accuracy of the walking speed estimates. It is a subject of our future study to quantitatively analyze how the error of the walking speed affects the assessment of the physical conditions of the seniors.

7. Conclusion

In this study, we have proposed a new algorithm, STZC, to estimate the gait speed of a human subject based on a Doppler radar system. Unlike the previously proposed STFT method that obtains the speed estimate through the frequency domain analysis, the STZC produces the estimate in the time domain through identifying the zero-crossing locations and an interquartile filter. The proposed STZC offers more robust and accurate estimates, whose performance is validated through experiments in the laboratory and in the senior residences. A single Doppler radar can only provide the velocity component along the direction between the subject and the radar. Future research would be to investigate the use of multiple Doppler radars and their optimum placements for gait speed estimation in elder care.

Acknowledgement

Research supported in part by the Agency for Healthcare Research and Quality under Grant R01HS018477.

References

[1] J.K. Aggarwal and Q. Cai, Human motion analysis: A review, *Computer Vision and Image Understanding* **73** (1999), 90–102.

[2] M. Alwan and R.A. Felder, *Eldercare Technology for Clinical Practitioners*, Humana Press, Totowa, NJ, 2008.

[3] M. Anderson and R. Rogers, Micro-Doppler analysis of multiple frequency continuous wave radar signatures, in: *Proceedings of SPIE Radar Sensor Technology*, Orlando, Florida, 2007, pp. 654–670.

[4] T. Banerjee, J. Keller, M. Skubic and E. Stone, Day or night activity recognition from video using fuzzy clustering techniques, *IEEE Transactions on Fuzzy Systems* **22** (2013), 483–493. doi:10.1109/TFUZZ.2013.2260756.

[5] I. Bilik, J. Tabrikian and A. Cohen, GMM-based target classification for ground surveillance Doppler radar, *IEEE Transcations on Aerospace Electronic Systems* **42** (2006), 267–278. doi:10.1109/TAES.2006.1603422.

[6] B. Boashash, Estimating and interpreting the instantaneous frequency of a signal-II: Algorithms and applications, *Proceedings of the IEEE* **80** (1992), 540–568. doi:10.1109/5.135378.

[7] J.J. Brunnekreef, C.J. Van Uden, S. Van Moorsel and J.G. Kooloos, Reliability of videotaped observational gait analysis in patients with orthopedic impairments, *BMC Musculoskeletal Disorders* **16** (2005), 17–25. doi:10.1186/1471-2474-6-17.

[8] R. Camicioli, D. Howieson, B. Oken, G. Sexton and J. Kaye, Motor slowing precedes cognitive impairment in the oldest old, *Neurology* **50** (1998), 1496–1498. doi:10.1212/WNL.50.5.1496.

[9] P. Cuddihy, T. Yardibi, Z.J. Legenzoff, L. Liu, C. Phillips II, C. Abbott, C. Galambos, J. Keller, M. Popescu, J. Back, M. Skubic and M. Rantz, Radar walking speed measurements of seniors in their apartments: Technology for fall prevention, in: *Proceedings of IEEE Engineering in Medicine and Biology Society*, San Diego, California, 2012, pp. 260–263.

[10] G. Demiris, M. Rantz, M. Aud, K. Marek, H. Tyer, M. Skubic and A. Hussam, Older adults' attitudes towards and perceptions of 'Smarthome' technologies: A pilot study, *Medical Informatics and the Internet in Medicine* **29** (2004), 87–94. doi:10.1080/14639230410001684387.

[11] DI-710 data logger manual (2013, Apr. 1) [Online]. Available at http://www.dataq.com/products/di-710.

[12] B. Dunmire, K.W. Beach, K.-H. Labs, M. Plett and D.E. Strandness Jr., Cross-beam vector Doppler ultrasound for angle independent velocity measurements, *Ultrasound in Medicine and Biology* **26** (2000), 1213–1235. doi:10.1016/S0301-5629(00)00287-8.

[13] J.L. Geisheimer, E.F. Greneker and W.S. Marshall, High-resolution Doppler model of the human gait, in: *Proceedings SPIE Radar Sensor Technology and Data Visualization*, Orlando, Florida, 2002, pp. 8–18. doi:10.1117/12.488286.

[14] B.R. Green, A. O'Donovan, R. Romero-Ortuno, L. Cogan, C.N. Scanaill and R.A. Kenny, Quantitative falls risk assessment using the timed up and go test, *IEEE Transactions on Biomedical Engineering* **57** (2010), 2918–2926. doi:10.1109/TBME.2010.2083659.

[15] I. Haritoglu, D. Harwood and L.S. Davis, W4: Real-time surveillance of people and their activities, *IEEE Transactions on Pattern Analysis and Machine Intelligence* **22** (2000), 809–830. doi:10.1109/34.868683.

[16] D. Hodgins, The importance of measuring human gait, *Medical Device Technology* **19** (2008), 44–47.

[17] B. Jansen, F. Temmermans and R. Deklerck, 3D human pose recognition for home monitoring of elderly, in: *Proceedings of 29th Annual International Conference of the IEEE Engineering in Medicine and Biology Society*, Lyon, France, 2007, pp. 4049–4051.

[18] Y. Kim and H. Ling, Human activity classification based on micro-Doppler signatures using a support vector machine, *IEEE Transcations on Geoscience and Remote Sensing* **47** (2009), 1328–1337. doi:10.1109/TGRS.2009.2012849.

[19] D.E. Krebs, J.E. Edelstein and S. Fishman, Reliability of observational kinematic gait analysis, *Physical Therapy* **65** (1985), 1027–1033.

[20] J. Li and H. Ling, ISAR feature extraction from non-rigid body targets using adpative chirplet signal representation, in: *Proceedings of IEEE Antennas and Propagation Society International Symposium*, San Antonio, Texas, 2002, pp. 294–297.

[21] Y. Li, K.C. Ho and M. Popescu, Efficient source separation algorithms for acoustic fall detection using a Microsoft Kinect, *IEEE Transactions on Biomedical Engineering* **61** (2014), 745–755. doi:10.1109/TBME.2013.2288783.

[22] B.E. Maki, Gait changes in older adults: Predictors of falss or indicators of fear, *Journal of the American Geriatrics Society* **45** (1997), 313–320. doi:10.1111/j.1532-5415.1997.tb00946.x.

[23] T.B. Moeslund, A. Hilton and V. Kruger, A survey of advances in vision-based human motion capture and analysis, *Computer Vision and Image Understanding* **104** (2006), 90–126. doi:10.1016/j.cviu.2006.08.002.

[24] M. Montero-Odasso, M. Schapira, E.R. Soriano, M. Varela, R. Kaplan, L.A. Camera and L.M. Mayorga, Gait velocity as a single predictor of adverse events in healthy seniors aged 75 years and older, *Journals of Gerontology, Series A: Biological Sciences and Medical Sciences* **60** (2005), 1304–1309. doi:10.1093/gerona/60.10.1304.

[25] M. Otero, Application of a continuous wave radar for human gait recognition, in: *Proceedings of SPIE Signal Processing, Sensor Fusion, Target Recognition*, Orlando, Florida, 2005, pp. 538–548.

[26] C.E. Phillips II, J. Keller, M. Popescu, M. Skubic, M.J. Rantz, P.E. Cuddihy and T. Yardibi, Radar walk detection in the apartments of elderly, in: *Proceedings of IEEE Engineering in Medicine and Biology Society*, San Diego, California, 2012, pp. 5863–5866.

[27] D. Podsiadlo and S. Richardson, The timed up and go: A test of basic functional mobility for frail elderly persons, *Journal of the American Geriatrics Society* **39** (1991), 142–148. doi:10.1111/j.1532-5415.1991.tb01616.x.

[28] M.J. Rantz, M. Skubic, C. Abbott, C. Galambos, Y. Pak, D. Ho, E. Stone, L. Rui, J. Back and S. Miller, In-home fall risk assessment and detection sensor system, *Journal of Gerontological Nursing* **39** (2013), 18–22. doi:10.3928/00989134-20130503-01.

[29] RCR50 manual (2013, Apr. 1) [Online]. Available at http://www.interlogix.com/_/assets/library/1036806B_RCR50_inin.pdf.

[30] L.N. Ridenour, Radar system engineering, *MIT Radiation Lab Series* **1** (1947), 629.

[31] M. Runger and G. Hunter, Determinants of musculoskeletal frailty and the risk of falls in old age, *Journal of Musculoskeletal and Neuronal Interactions* **6** (2006), 167–173.

[32] P. Setlur, M. Amin and F. Ahmad, Urban target classifications using time-frequency micro Doppler signatures, in: *Proceedings of International Symposium of Signal Processing and Its Application*, Sharjah, UAE, 2007, pp. 1–4.

[33] T. Shiraishi et al., Indoor location estimation technique using UHF band RFID, in: *Proceedings of International Conference on Information Networking*, Busan, Korea, 2008, pp. 1–5.

[34] G.E. Smith, K. Woodbridge and C.J. Baker, Template based micro-Doppler signature classification, in: *Proceedings of European Radar Conference*, Manchester, UK, 2006, pp. 158–161.

[35] E. Stone and M. Skubic, Evaluation of an inexpensive depth camera for in-home gait assessment, *Journal of Ambient Intelligence and Smart Environments* **3** (2011), 349–361.

[36] E. Stone and M. Skubic, Unobtrusive, continuous, in-home gait measurement using the Microsoft Kinect, *IEEE Transactions on Biomedical Engineering* **60** (2013), 2925–2932. doi:10.1109/TBME.2013.2266341.

[37] E. Stone, M. Skubic, M. Rantz, C. Abbott and S. Miller, Average in-home gait speed: Investigation of a new metric for mobility and fall risk assessment of elders, *Gait and Posture* **41** (2015), 57–62. doi:10.1016/j.gaitpost.2014.08.019.

[38] T.H. Tan, M. Gochoo, K.H. Chen, F.R. Jean, Y.F. Chen, F.J. Shih and C.F. Ho, Indoor activity monitoring system for elderly using RFID and Fitbit flex wristband, in: *Proceedings of International Conference on Biomedical and Health Informatics*, Valencia, Spain, 2014, pp. 41–44.

[39] T. Thayaparan, S. Abrol, E. Riseborough, L. Stankovic, D. Lamothe and G. Duff, Analysis of radar micro-Doppler signatures from experimental helicopter and human data, *IET radar, Sonar, Navigation* **1** (2007), 289–299. doi:10.1049/iet-rsn:20060103.

[40] P. Tortoli, G. Bambi and S. Ricci, Accurate Doppler angle estimation for vector flow measurements, *IEEE Transactions on Ultrasonic, Ferroelectrics, and Frequency Control* **53** (2006),

1425–1431. doi:10.1109/TUFFC.2006.1665099.

[41] S. Vasunilashorn, A.K. Coppin, K.V. Patel, F. Lauretani, L. Ferrucci, S. Bandinelli et al., Use of the short physical performance battery score to predict loss of ability to walk 400 meters: Analysis from the InCHIANTI study, *Journal of Gerontology, Series A: Biological Sciences and Medical Sciences* **64** (2009), 223–229. doi:10.1093/gerona/gln022.

[42] Vicon Bonita manual (2013, Apr. 1) [Online]. Available at http://www.vicon.com/System/Bonita.

[43] F. Wang, M. Skubic, M. Rantz and P. Cuddihy, Quantitative gait measurement with pulse-Doppler radar for passive in-home gait assessment, *IEEE Transactions on Biomedical Engineering* **61** (2014), 2434–2443. doi:10.1109/TBME.2014.2319333.

[44] F. Wang, E. Stone, M. Skubic, J. Keller, C. Abbott and M. Rantz, Towards a passive low-cost in-home gait assessment system for older adults, *IEEE Journal of Biomedical and Health Informatics* **17** (2013), 346–355. doi:10.1109/JBHI.2012.2233745.

[45] T. Yardibi, P. Cuddihy, S. Genc, C. Bufi, M. Skubic, M. Rantz, L. Liu and C. Phillips II, Gait characterization via pulse-Doppler radar, in: *Proceedings of IEEE International Conference on Pervasive Computing and Communications Workshops*, Seattle, WA, 2011, pp. 662–667.

[46] Z. Zhou, X. Chen, Y.C. Chung, Z. He, T.X. Han and J.M. Keller, Activity analysis, summarization and visualization for indoor human activity monitoring, *IEEE Transactions on Circuits and Systems for Video Technology* **18** (2008), 1489–1498. doi:10.1109/TCSVT.2008.2005612.